Comparison of proton irradiated P-channel and N-channel CCDs

Journal Item

Comparison of Proton Irradiated P-channel and N-channel CCDs

Jason P. D. Gow [a,*] Neil J. Murray [a] Andrew D. Holland [a]
David Burt [b] Peter J. Pool [b]

[a] *e2v centre for electronic imaging, Planetary and Space Sciences, The Open University, Walton Hall, Milton Keynes MK7 6AA, UK*

[b] *e2v technologies plc, 106 Waterhouse Lance, Chelmsford, Essex, CM1 2QU, UK*

Abstract

Charge transfer inefficiency and dark current effects are compared for e2v technologies plc. p-channel and n-channel CCDs, both irradiated with protons. The p-channel devices, prior to their irradiation, exhibited twice the dark current and considerable worse charge transfer inefficiency (CTI) than a typical n-channel. The radiation induced increase in dark current was found to be comparable with n-channel CCDs, and its temperature dependence suggest the divacancy is the dominant source of thermally generated dark current pre and post irradiation. The factor of improvement in tolerance to radiation induced CTI varied by between 15 and 25 for serial CTI and 8 and 3 for parallel CTI, between -70 °C and -110 °C respectively.

Key words: Image sensors, CCD, proton radiation effects, p-channel, CTI, CTE

1 Introduction

The most abundant charged particle within the space radiation environment is the proton [1]. It has long been established that for charge coupled devices (CCDs) the main source of damage arises from protons within the Earth′s radiation belts and cosmic rays [2,3]. Protons cause displacement damage within the silicon lattice, generating stable defects and thereby creating energy levels within the silicon band-gap [4]. In n-channel CCDs the dominant traps

* Corresponding author:
Email address: j.p.d.gow@open.ac.uk (Jason P. D. Gow).

pre-irradiation have energies of 0.12 and 0.30 eV below the conduction band [5]. The former is thought to be the oxygen-vacancy (A-centre), the origin of the latter is unknown but is thought to be vacancy related. Post-irradiation the density of these traps increases and an additional trap is generated with an energy of around 0.42 eV below the conduction band, attributed to the phosphorous-vacancy (E-centre). The emission time of the E-centre is comparable to the clock periods typically used in CCD operation, thus making it the dominant defect for decreasing the charge transfer efficiency (CTE) in n-channel CCDs. The effect is often described by the charge transfer inefficiency (CTI), where CTI = 1 - CTE, because it increases linearly with proton fluence [6] and can also be described by the radiation damage constant (RDC).

A number of methods can be employed to minimise the increase in CTI, such as including a supplementary buried channel, providing a high temperature anneal while in orbit, or increasing the shielding [6]. It has been suggested and demonstrated [7] that with a p-channel CCD the density of radiation induced traps is lower than with n-channel, thereby reducing the post irradiation increase in CTI.

A number of problems do however arise when trying to compare CTI measurements between n-channel and p-channel CCDs. These can be due to different operating conditions, different CTI analysis techniques, and differing device structure [8]. The aim of this study was to compare the post irradiation dark current and CTI of a p-channel e2v technologies plc. CCD47-20 [9], with the detailed analysis performed on n-channel e2v technologies plc. CCD02s [3,5,10] under the same operating conditions, including incident X-ray flux.

Whereas the dominant trap types in n-channel CCDs are well documented [2,3,5,11–13], less is known about the traps to be expected in p-channel CCDs. A major trap is likely to be the divacancy with an energy around 0.18 eV [14] to 0.21 eV [15] above the valance band , other traps could be related to carbon and oxygen interstitials [16].

2 Experimental

The CCD47-20 under test was a front-illuminated frame transfer device with an image and store format of 1024 by 1024, and 13 µm square pixels. It should be noted that the same clocking scheme was used to read out the image and store regions. The p-type buried channel was doped with boron, the epitaxial layer with phosphorous (20 to 100 Ω.cm), and the substrate with antimony (<20 mΩ.cm). The dopants were selected to provide comparable resistivity and properties to those found in n-channel devices with minimal dopant induced

lattice stress [9]. The concentration of phosphorous is two orders of magnitude lower than that in n-channel devices, therefore the formation of E-centre defects will be negligible [9]. The CCD02 is a front illuminated device, with an image format of 385 by 578, and 22 µm square pixels.

The CCD47 was clamped onto a copper cold bench connected to a CryoTiger refrigeration system (PT-30) with thermal control provided using a resistive heater in thermal contact with the copper cold bench. Data collected above -40 °C were recorded while the CCD47 was cooled, with the heater at maximum to reduce the rate of cooling. Temperature control was provided to within ± 0.1 °C using a feedback system, composed of a Lakeshore 325 temperature controller, the heater, and a 1,000 Ω platinum resistance thermometer mounted on the device ceramic. It is assumed that the device silicon is in good thermal contact with the ceramic. An Oxford Instruments XTF5011/75-TH X-ray tube, with a tungsten anode, was used to fluoresce a manganese target held at 45° to the incident X-ray beam to provide a known energy (5,898 eV) for calibration and CTI measurements. The X-ray tube was powered down during CCD47 read-out. Clocking and biasing was provided by an XCAM ltd. USB2REM1 camera drive box in conjunction with USB2 v1.15 drive software.

The mean dark current was measured between 0.0 °C and -110.0 °C, and the CTI was measured using the X-ray technique between -40.0 °C and -110.0 °C. Only events identified as isolated using a threshold of 9σ, where σ is the standard deviation of the noise peak, were used during CTI analysis. The RDC, given by equation 1, was used to make the comparison to the n-channel CCD02. The n-channel CCD02 RDC was normalised to that of the p-channel CCD, for parallel and serial respectively, by accounting for the different pixel geometries (pixel length, buried channel width, and an assumption on fringing fields). It should be noted that as a result of increased CTI the image area used for CTI analysis was reduced in the irradiated CCD47s as X-ray events could not be identified, i.e. they were spread over multiple pixels as a result of poor CTE.

$$RDC = \frac{\Delta CTI}{10MeVprotonfluence} \tag{1}$$

2.1 Proton Irradiation

The proton irradiation was performed at the Paul Scherrer Institut (PSI) in Switzerland, with six p-channel and two n-channel CCD47-20s. The entire active area of the devices were irradiated using 63 MeV protons, with one device held as a control, the irradiation details are given in Table 1. During initial testing, performed by e2v technologies plc, the parallel and serial CTI

Table 1
Irradiation characteristics for the p-channel CCD47-20s irradiated at PSI

Device	**Beam Energy (MeV)**	**Flux ($cm^{-2}.s^{-1}$)**	**Fluence (cm^{-2})**	**10 MeV Equivalent Fluence (cm^{-2})**
×3	63	1.70×10^{8}	2.70×10^{11}	1.35×10^{11}
×3	63	1.40×10^{8}	8.12×10^{10}	4.07×10^{10}
×1	Not irradiated			

of the p-channel and n-channel devices were measured using Mn-K_α X-rays at -30 °C and -50 °C [9]. The n-channel CCD47s underwent an anneal stage, and as a result were not used for comparison in this study.

3 Results and Discussion

3.1 Dark Current

The dark current data collected from the devices tested were plotted in an Arrhenius plot, illustrated in Figure 1 [17] for three devices pre and post-irradiation, with a fit to data points recorded above -51 °C (4.5×10^{3} K^{-1}). Below -55 °C the data points no longer follow the exponential fit. The plateau below -77 °C (5.1×10^{3} K^{-1}) is believed to show the limit of the measurement technique, where insufficient dark current was generated to be measured, requiring a longer integration time. Using the approximation from equation 2, where A is some constant, E_{act} is the activation energy, k is Boltzmanns constant and T is the temperature [13]. E_{act} was calculated to be 0.61 eV pre-irradiation, 0.62 eV after irradiation with 4.07×10^{10} protons.cm^{-2}, and 0.63 eV after irradiation with 1.35×10^{11} protons.cm^{-2}, corresponding to trap energies of about 0.49, 0.48, and 0.47 eV, respectively.

$$Dark\ Current = Aexp(\frac{-E_{act}}{kT}) \tag{2}$$

The results are comparable to other reported values of activation energies of 0.61 eV [15] and 0.63 eV [18]. The measurement suggests that, for the p-channel devices tested, the divacancy is the dominant source of thermally generated dark current pre and post irradiation.

At 20 °C the irradiated CCD47s were saturated with dark current, so the dark current at this reference temperature was calculated using the equations of the lines of best fit. The increase in dark current at 20 °C was calculated to be ∼1.2 nA.cm^{-2}.$krad^{-1}$, similar to other e2v n-channel CCDs [13]. The un-irradiated dark current was calculated to be ∼2.5 nA.cm^{-2} at 20 °C, over

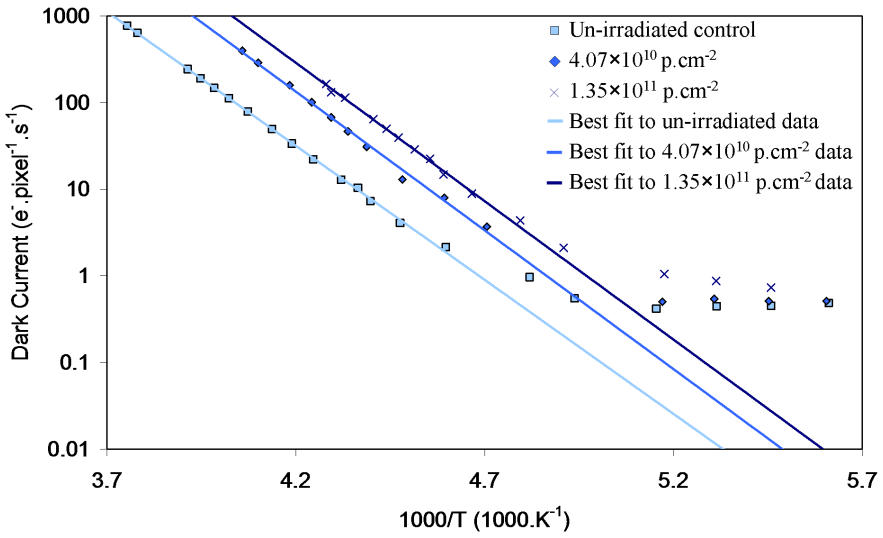

Fig. 1. Dark current as a function of 1000/T for three p-channel devices pre and post-irradiation with protons [17]

twice the typical value of ∼1 nA.cm^{-2} for n-channel CCDs, this is likely to be the result of the silicon selected. Unfortunately the devices were not available for testing prior to the irradiation, so no comparison could be made on the rate of hot pixel generation.

3.2 Charge Transfer Inefficiency

The poor pre-irradiation CTI performance is attributed to the silicon selected and device fabrication on epitaxial silicon. Bulk (float zone) devices [15,19] have demonstrated equivalent CTI to n-channel CCDs, the next generation of p-channel CCDs will be fabricated on bulk silicon. The temperature dependence of parallel and serial CTI for the un-irradiated and a device irradiated CCDs is shown in Figures 2 and 3 respectively. The trend for both irradiated and un-irradiated devices demonstrate an increase in CTI as they are cooled between -40 °C and -60 °C, attributed to the decrease in the number of thermally generated holes filling traps. The lower amount of charge per unit volume per unit time travelling in the parallel direction, when compared to the serial direction, leads to parallel CTI being more effectively recovered using charge injection within the imaging area. As a result the increase in parallel CTI observed in Figure 2 between -40 °C and -60 °C is greater than the increase observed in serial CTI in Figure 3.

The emission time constant, τ_e, of some hole defects are illustrated in Figure 4, calculated using values reported by Mostek *et al.* [14]. The resulting spread from the errors on the measurement, the time allowed for the charge to rejoin the charge packet, t_r, and the mean time between successive X-ray events,

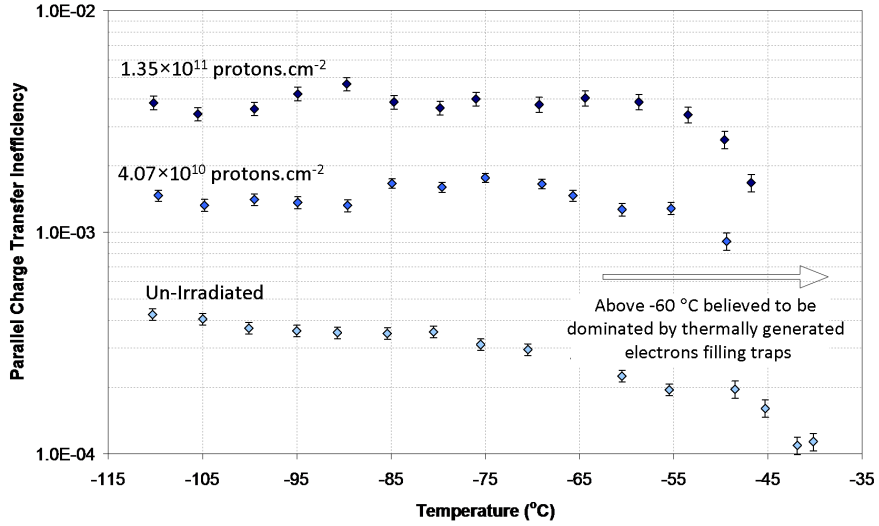

Fig. 2. Parallel charge transfer inefficiency as a function of temperature for an un-irradiated CCD and a CCD irradiated with a 10 MeV proton fluence of 4.07×10^{10} and 1.35×10^{11} protons.cm^{-2}.

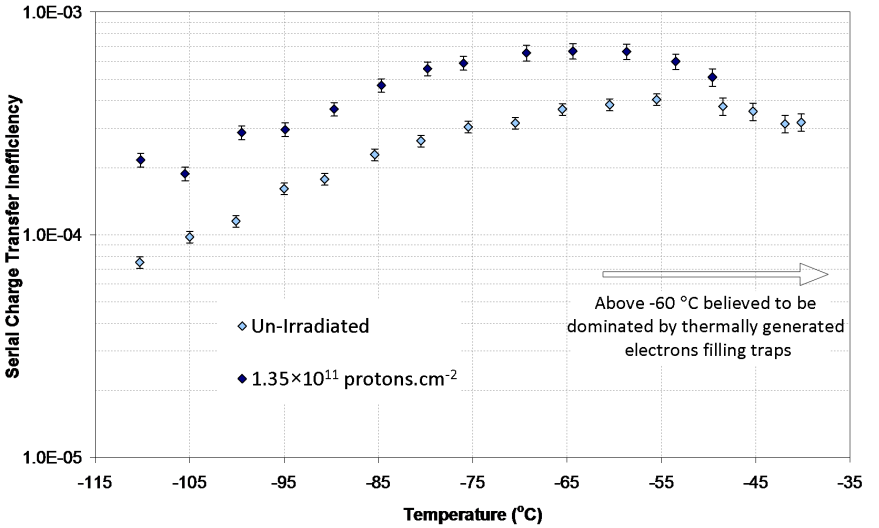

Fig. 3. Serial charge transfer inefficiency as a function of temperature for an un-irradiated CCD and a CCD irradiated with a 10 MeV proton fluence of 1.35×10^{11} protons.cm^{-2}.

t_x, are also illustrated. The CTI will be low if the τ_e is very much less than t_r, a high probability that charge can rejoin the charge packet, and if τ_e is very much greater than t_x, a high probability that the traps will remain filled effectively frozen out. Therefore a defect with a τ_e between t_r and t_x will have a significant influence on the measured CTI.

Below -60 °C the parallel CTI of the un-irradiated device continues to increase with decreasing temperature, indicating that another defect is becoming more effective, possibly the C_iO_i defect with a small contribution from the

C_i defect [14]. It should be noted that the devices spent around 1 year at room temperature prior to the analysis, over which time the C_i defects would be mobile [20], leaving few C_i defects remaining [14]. The parallel CTI measurements in Figure 2 below -60 °C are almost featureless, with no clear trends associated with point defects. Over the measured temperature range Figure 4 suggests that the C_iO_i defect will have the greatest impact of parallel CTI, with only a negligible contribution from the other defects, therefore the effect on parallel CTI could be small. The errors on these measurements could result in a small trend being lost within the error, the increase in error arises from the accuracy of the peak fitting routine which is dependant on the number of X-ray events available for analysis which in cases of poor CTI is reduced, due to charge trailing over multiple pixels. Until pocket pumping is performed using the p-channel CCD47 no conclusive explanation of the lack of features can be provided.

The serial CTI decreases with a similar trend for both the un-irradiated and irradiated devices, as illustrated in Figure 3, as the τ_e of the C_iO_i defect increases above t_x. The data points at around -105 °C and -110 °C, for the irradiated devices may indicate an end to the improvement, possibly as a result of the divacancy τ_e approaching t_r. The effect was observed in all of the irradiated CCDs and became more prominent with increasing proton fluence, it was not observed in the un-irradiated CCD. It is tempting to say that the effect is as a result of the increase in radiation induced divacancy defects and that the divacancy defect had a negligible affect on the temperature dependence of serial CTI pre-irradiation, however only one un-irradiated device was available for testing.

3.3 Comparison with an n-channel CCD

The CTI was measured at -70 °C, -90 °C, and -110 °C to identify the temperature dependence of the improvement in radiation tolerance to radiation induced CTI of the p-channel CCDs under test, the results are illustrated in Figure 5. In the case of the devices examined within this study, cooling the CCD47 reduces the increased radiation tolerance afforded by a p-channel CCD for parallel transfers as a result of the n-channel E-centre defects becoming permanently filled. Serial transfers continued to benefit from further cooling as the τ_e increases over the t_x. The base performance of the p-channel devices tested was poor when compared the n-channel CCD02, making it essential that for practical CCD applications the baseline performance of these p-channel CCDs be improved.

It should be noted that the e2v test results at -30 °C and -50 °C indicated an improvement in radiation tolerance of a factor >3 in serial CTI and less

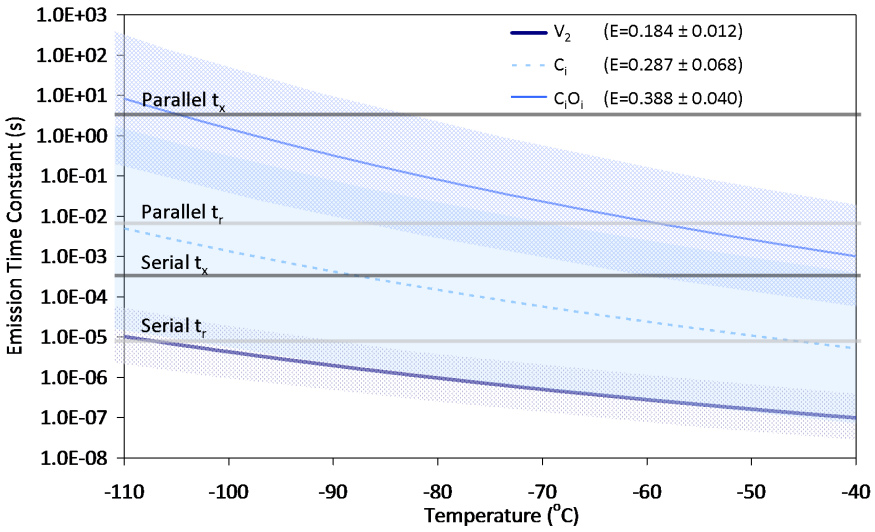

Fig. 4. Emission time constants of the divacancy, carbon interstitial (C_i), and the carbon-oxygen (C_iO_i) defects as a function of temperature taken from values given in the literature, the shaded regions illustrate the effect of the reported errors [14]. The time between successive X-ray events and the time allowed for charge to rejoin the charge packet are illustrated for serial and parallel transfers.

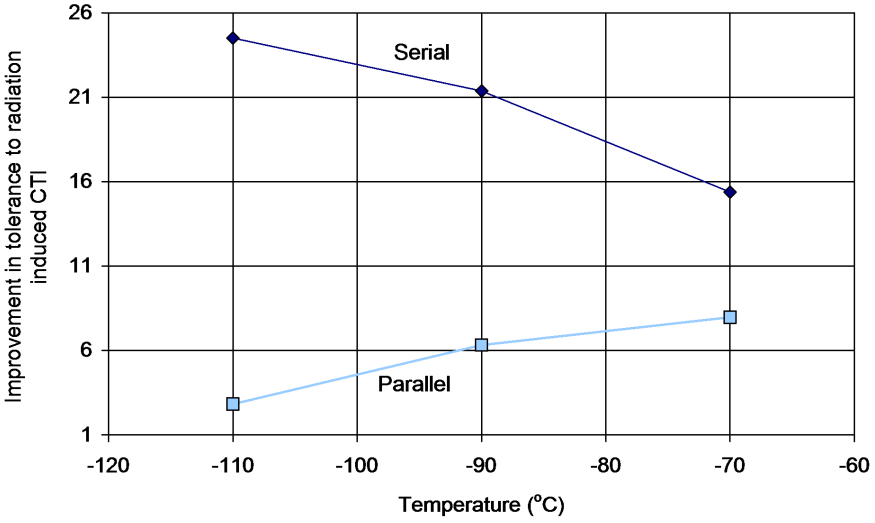

Fig. 5. Improvement in tolerance to radiation induced parallel and serial CTI as a function of temperature.

for parallel [9]. These results highlight the importance of measuring the CTI effects over a range of temperatures due to the temperature dependence of defect behaviour.

A comparison of the measured p-channel performance, and calculated n-channel performance, accounting for the different pixel geometries, is illustrated in Figure 6 for parallel CTI at -70 °C. The estimation of the volume available for charge transport was made using the parallel and serial channel

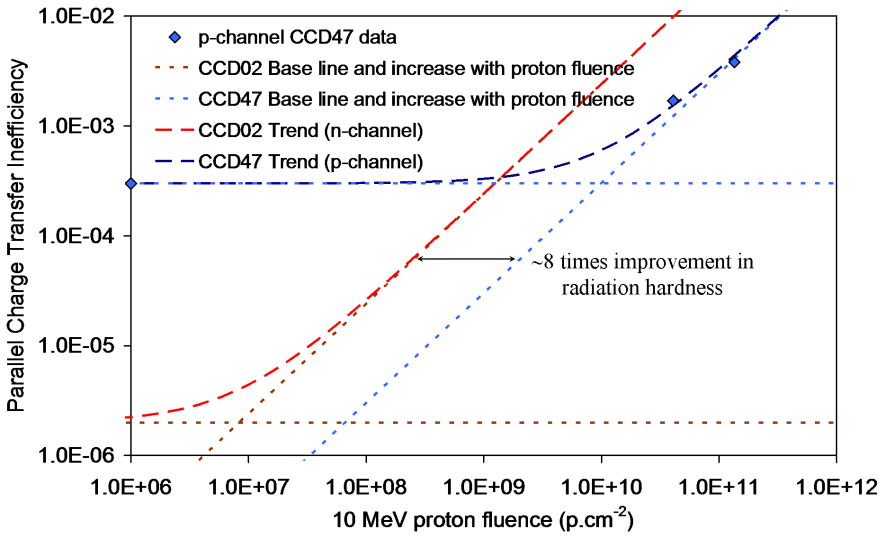

Fig. 6. Comparison of the p-channel CCD47 with an n-channel CCD02 at -70 °C showing the ×8 improvement in radiation tolerance.

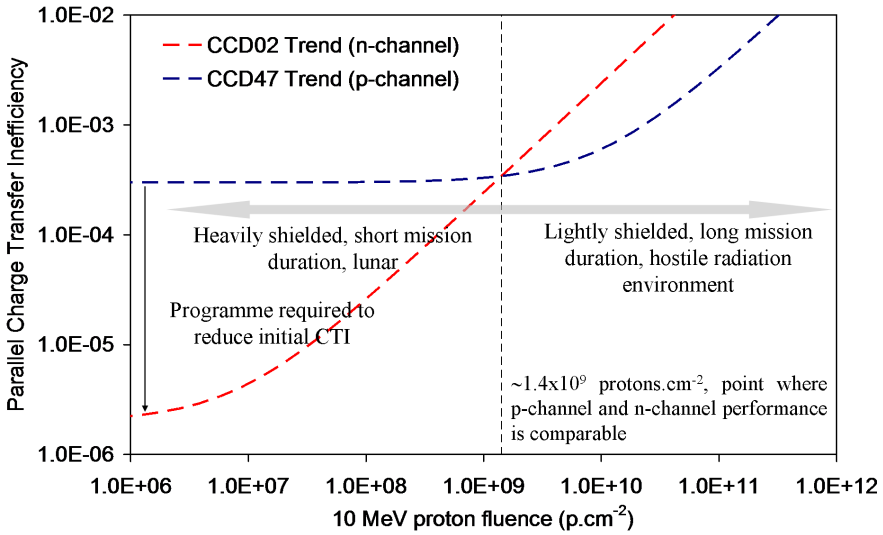

Fig. 7. Comparison of the p-channel CCD47 with an n-channel CCD02 at -70 °C showing the operational suggestions for a p-channel CCD47 at its current level of performance.

widths, pixel length and an assumption on fringing fields. The un-irradiated baseline and CTI values calculated using the appropriate RDC values are illustrated and were used to provide a fit to the p-channel data. Despite being a factor of 8 times more tolerant to radiation induced parallel CTI, the p-channel CCD47 under test would only outperform the n-channel CCD02 after a 10 MeV equivalent proton fluence of $\sim 1.4 \times 10^9$ protons.cm^{-2} because of the poor initial performance, illustrated in Figure 7.

4 Conclusion

The p-channel CCD47 exhibited twice the un-irradiated dark current of a typical e2v n-channel CCD, while the radiation induced rate of increase was comparable. The temperature dependence indicates a mid-band defect with an activation energy of around 0.62 eV is responsible for the thermally generated dark current, comparable to other reported values and attributed to the divacancy [21].

The initial serial and parallel CTI was high when compared to n-channel performance, this was attributed to the silicon selected and device fabrication on epitaxial silicon. Bulk (float zone) devices have demonstrated base CTI equivalent to n-channel devices [15,19] and will be used during the fabrication of future p-channel devices. The comparison with n-channel performance demonstrates a temperature-dependant improvement in the tolerance to radiation induced CTI. It should be noted that until devices are fabricated using the same mask set, operated using the same timings, and analysed using the same method, any comparison should be viewed with caution.

Despite the poor initial CTI, the large improvement in tolerance to radiation-induced CTI still makes these devices, at their current level of performance, suitable for use in hostile radiation environments, indicating that such p-channel devices will have a large part to play in the future of CCDs in space. A future study using these CCDs will more fully investigate the defects through the use of pocket pumping, and a new study will be performed on n-channel and p-channel CCDs fabricated on the same mask set and operated under the same conditions.

Acknowledgment

The authors would like to thank ESA for providing the devices, Mark Robbins, James Endicott, Andrew Pike, and John Turton of e2v, and David Hall of the centre for electronic imaging for their support during this programme.

References

[1] E. G. Stassinopoulos, and J. P. Raymond, Proc. of the IEEE vol. 76 (1988) 1423-1442.

[2] C. Janesick, IEEE Trans. Nucl. Sci. vol. 36, (1989) 572-578.

[3] A. Holmes-Siedle, A. Holland, and S. Watts, IEEE Trans. Nucl. Sci. vol. 43 (1989) 2998-3004.

[4] J. R. Srour, C. J. Marshall, and P. W. Marshall, IEEE Trans. Nucl. Sci. vol. 50 (2003) 653-670.

[5] A. Holland, Nucl. Inst. Meth. A326 (1993) 335-343.

[6] A. Holland, et al., IEEE Trans. Nucl. Sci. vol. 38 (1991) 1663-1670.

[7] J. P. Spratt, B. C. Passenheim, and R. E. Leadon, IEEE Radiation effects data Workshop (1997) 116-121.

[8] D. H. Lumb, Proc. SPIE vol. 7439 (2009).

[9] B. de Monte, et al., "Proton Irradiation Test Summary Report", e2v technologies plc. internal report, 2008.

[10] CCD02 data sheet, e2v technologies plc.

[11] G. D. Watkins and J. W. Corbett, Phys. Rev. vol. 134 no. 5A (1964) 1359-1377.

[12] A. S. Grove, 'Physics and Technology of Semiconductor Devices', Wiley, 1967.

[13] G. R. Hopkinson, C. J. Dale, and P. W. Marshall, IEEE Trans. Nucl. Sci. vol. 43 (1996) 614-627.

[14] N. J. Mostek, et al., Proc. SPIE vol. 7742 (2010).

[15] C. Bebek, et. al., IEEE Trans. Nucl. Sci. vol. 49 (2002) 1221-1225.

[16] M. Moll, "Radiation damage in silicon particle detectors", Ph.D. dissertation, Physics Dept., Univ. of Hamburg, Germany, 1999.

[17] J. Gow, et all, Proc. SPIE vol. 7435 (2009).

[18] J. P. Spratt, et al., IEEE Trans. Nucl. Sci. vol. 52 (2005) 2695-2702.

[19] K. Dawson, et. al., IEEE Trans. Nucl. Sci. vol. 55 (2008) 1725-1735.

[20] M. R. Brozel, R. C. Newman, and D. H. J. Totterdell, J. Phys. C: Solid State Phys. vol. 8 (1975).

[21] J. R. Srour, IEEE Trans. Nucl. Sci. vol. 47 (2000) 2451-2459.